AIChE

Impact of Retention on Trans-Column Velocity Biases in Packed Columns

Fabrice Gritti and Georges Guiochon
Dept. of Chemistry, University of Tennessee, Knoxville, TN 37996

DOI 10.1002/aic.12074
Published online December 14, 2009 in Wiley InterScience (www.interscience.wiley.com).

The heights equivalent to a theoretical plate of a weakly and strongly retained compounds were measured on two packed columns having different average mesopore sizes. The measurements were carried out in two different cases, with access to the mesopores by the sample molecules blocked (filled with n-nonane) or not. The experimental results demonstrate that the eddy dispersion terms of both columns are significantly smaller for porous than for nonporous particles. Two simultaneous phenomena explain this observation. First, packed columns are radially heterogeneous which causes significant trans-column velocity biases warping the bands. Second, radial dispersion contributes to mass transfer across the column, relaxing the radial concentration gradients that are caused by these velocity biases. The impact of these biases is minimized when the pores of the particles are not blocked; it decreases with increasing residence time and radial dispersion coefficient of the solutes. © 2009 American Institute of Chemical Engineers *AIChE J,* 56: 1495–1509, 2010

Keywords: liquid chromatography, column efficiency, mass transfer kinetics, parking experiments, longitudinal diffusion coefficient, particle diffusivity, total pore blocking experiments, eddy dispersion, transcolumn eddies, soid-liquid mass transfer resistance, film mass transfer, Sherwood number, transparticle mass transfer resistance, porous and nonporous particles

Introduction

The performance of 1D and 2D liquid chromatography processes relies on the efficiency of the columns used. In RPLC, when frictional heating is negligible, the mass transfer kinetics of small molecules at high flow rates is essentially controlled by flow heterogeneity in the packed bed (the *A* term) and by the film mass transfer resistance between the moving eluent in the interstitial volume and the stagnant eluent inside the mesopores of the porous particles (part of the overall *C* term) (Gritti F, Guiochon G. New insights on mass transfer kinetics in chromatography submitted). The longitudinal diffusion term (*B*) is negligible at high reduced linear velocities *v*. The mass transfer resistance of the sample molecules through the porous particles is also negligible because surface diffusion accelerates considerably the effective diffusivity of these molecules through the particles. Surface diffusion far outpaces pore diffusion and accounts for at least 80% of the overall particle diffusivity,[1] which is not yet realized by chromatographers but explains most of the success of modern RPLC packing materials for the separation and/or the purification of most retained small molecules. This is also true with larger molecules such as insulin for which surface diffusion accounts for more than 95% of the total particle diffusivity.[2]

Eddy dispersion and film mass transfer resistance are the only factors limiting the performance of RPLC columns in fast chromatography, provided that the heat power released by friction[3,4] be smaller than 4 W per meter of column length.[5] If frictional heating takes place, an additional term accounting for band broadening due to a radial temperature gradient should be added.[6]

The film mass transfer coefficient, k_f, can be accurately estimated for nonporous spherical particles. The Wilson &

Correspondence concerning this article should be addressed to G. Guiochon at guiochon@utk.edu

Geankoplis correlation[7] was recently validated in liquid chromatography for a column packed with 18 μm nonporous C_{18} -bonded particles.[8] Yet, the validity of this equation was recently questioned for columns packed of porous particles, the general case of commercial columns (Gritti F, Guiochon G. New insights on mass transfer kinetics in chromatography submitted). An analysis of the experimental *C*-term measured at reduced velocities $v > 15$ revealed that the film mass transfer coefficient was about half the value predicted by the Wilson & Geankoplis correlation. Because the external surface area of particles is a random distribution of solid/liquid (silica-C_{18}/moving eluent) and liquid/liquid (stagnant eluent/moving eluent) interfaces, the local sample concentration gradients in the vicinity of the solid phase (where adsorption/desorption actually takes place) are necessarily stronger than those close to the stagnant eluent (where diffusion in/out particles occurs). Actually, smaller effective film mass transfer coefficients were measured.

The eddy dispersion term of HETP equations is often considered as constant in liquid chromatography, and estimated to be close to two particle diameters. As shown by Giddings, this term includes the contributions of trans-channel ($h = 1$), short-range interparticle ($h = 0.9$), and long-range interparticle ($h = 0.1$) velocity inequalities.[9–12] The eddy dispersion term should a priori be the same for all solutes, whether excluded or not from the mesopore volume of the adsorbent and whether the compound is retained or not.[13,14] This assumption was recently challenged from an experimental point of view, on the basis of the important differences between the HETP of a column measured before and after blocking solute access to mesopores (Gritti F, Guiochon G. New insights on mass transfer kinetics in chromatography submitted). The overall eddy dispersion term of a retained solute was two to three times larger when it had no access to the mesopore volume than when it had access to them. Trans-column eddies were always suspected as be a source of band broadening in packed columns, as already observed in packed columns[15–18] and more recently in monolithic columns.[19–21] Still, this observation does not explain why the A-term is significantly higher when access to the mesopore volume is blocked. A new model of eddy dispersion is needed. The theoretical expression of the trans-channel, short-range interchannel, and long-range interchannel eddy dispersion contributions to the HETP are not questionable. Giddings' coupling theory of eddy dispersion matches fairly well experimental results.[22] Nevertheless, the derivation of the trans-column eddy term was dubious. For instance, the flow controlled reduced HETP term (at high v) is estimated at $2 \times 0.02\ m^2$, where m is the number of particle diameters across a column diameter.[11,12] In a 4.6-mm I.D. column packed with 5 μm particles, $m = 920$ and the trans-column reduced HETP should be equal to nearly 34,000! Although acceptable for open tubular columns (500 μm wide) packed with large particles (50 μm), this expression cannot hold in today's packed columns. A new model accounting for the observed trans-column eddies is needed.

The main goal of this work is to understand why columns packed with porous particles have a smaller eddy dispersion contribution to their HETP than those packed with nonporous particles. We measured the mass transfer resistance of a nonretained solute, thiourea, and that of a strongly retained one, phenol, in two commercial packed columns (150×4.6 mm, 5 μm particles, Jupiter-C_{18}, 300 Å pore size, and Luna(2)-C_{18}, 100 Å pore size, Phenomenex) before and after blocking access of these solutes to the mesopore volume. The reduced HETP data are compared, and the differences are analyzed and discussed. A theoretical interpretation of the results is proposed, based on the assumption that packed beds are radially heterogeneous and that trans-column eddies are responsible for the observations.

Theory

Definitions

The following terms will be used in this work.

The particle diffusivity D_p measures the effective diffusion coefficient of a compound across the individual particles of a packing material. The driving force of particle diffusion is the concentration gradient in the pores,[23] which is consistent with the definition of the effective particle diffusivity in the general rate model of chromatography.[24,25] Particle diffusivity results from the combination of pore and surface diffusion. The ratio of D_p and the molecular diffusivity, D_m, of a compound in the bulk mobile phase will be Ω.

The axial diffusion coefficient $D_{eff}(v = 0)$ of a compound is its effective diffusion coefficient inside the packed bed, at a zero mobile phase velocity. It is the apparent diffusion coefficient of the sample in the same column but filled with the bulk solution, only (no particles, $\varepsilon_e = 1$). It results from the combination of its molecular diffusivity in the interstitial column volume (D_m), the bed tortuosity, and the particle diffusivity (D_p). The ratio of $D_{eff}(v = 0)$ and the bulk diffusivity, D_m, is Ω_c.

The average radial diffusion coefficient $\overline{D}_r(v)$ of a compound across the column is its effective radial diffusion coefficient inside the packed bed when an interstitial linear velocity, u, is applied along the bed of packed particles of diameter d_p. It is expressed as the sum of a diffusive term ($D_{eff}(v = 0)$) and a convective term ($\propto u d_p$).

The trans-particle and the film mass transfer coefficients C_p and C_f of the general reduced plate height model are derived from the moments of the Laplace transform of the general rate model equations,[26–28] assuming the packed particles to be spherical.

General HETP equation for chromatographic columns

The broadening of a band migrating along an isothermal chromatographic column is due to the simultaneous influence of a series of independent processes. Giddings discussed in detail each of these mass transfer steps from a phenomenological point of view and provided the fundamentals of band broadening in chromatography.[11] These steps are axial diffusion of the band in the absence of flow or in the mobile phase reference framework, eddy dispersion in the interstitial void volume (interparticle space), mass transfer resistance through the thin film of eluent between the stream of eluent percolating the interstitial column volume, and the stagnant pool of eluent stagnant inside the porous adsorbent particles, the mass transfer resistance between the two eluents, the mass transfer resistance through the particles, and the kinetics of adsorption-desorption, which is usually very fast with small molecules and usually neglected. These different terms are accounted for by corresponding contributions to

the general rate model.[25] In the linear case, the set of mass balance equations of this model can be solved in the Laplace domain. However, this solution cannot be transformed back to the time domain, only its moments can. This provides the moments of the chromatographic band at the column outlet.[26] Application of this mathematical strategy was extended to other chromatographic bed structures (e.g., beds packed of fully, partially, or nonporous particles and monolithic beds). It lead to specific expressions valid in these cases.[28] Since longitudinal diffusion and eddy dispersion can be considered as independent kinetic phenomena, the overall reduced HETP of an isothermal column packed with fully porous spherical particles can be written as follows[11,25]:

$$h(v) = \frac{2D_{\text{eff}}(v)}{v} + h_{\text{eddy}}(v) + \frac{1}{30}\frac{\varepsilon_e}{1-\varepsilon_e}\left(\frac{\delta_0}{1+\delta_0}\right)^2 \frac{1}{\Omega} v + \frac{1}{3}\frac{\varepsilon_e}{1-\varepsilon_e}\left(\frac{\delta_0}{1+\delta_0}\right)^2 \frac{D_m}{k_f d_p} v \quad (1)$$

$$= \frac{2D_{\text{eff}}(v)}{v} + h_{\text{eddy}}(v) + C_p v + C_f v \quad (2)$$

where $D_{\text{eff}}(v)$ is the longitudinal diffusion coefficient, a function of the linear reduced velocity, v, $h_{\text{eddy}}(v)$ is the eddy dispersion term, ε_e is the interstitial porosity of the column, d_p is the average particle size, and k_f is the film mass transfer coefficient between the solid phase surface and the mobile phase. $\frac{k_f d_p}{D_m}$ is the dimensionless Sherwood number. The reduced interstitial linear velocity v is defined as:

$$v = \frac{u d_p}{D_m} \quad (3)$$

where u is the local interstitial linear velocity. The diffusion coefficients D_m of thiourea and phenol were derived from the reference experimental diffusion coefficient of thiourea measured in pure water and at 298 K[29,30] and from the analysis of the longitudinal diffusion coefficient by the peak parking method applied to adsorbent with the mesopores blocked by *n*-nonane. They will be compared to the estimates derived from the Wilke and Chang equation,[31] which provides reasonable estimates of the diffusion coefficient D_m of small analytes in the mobile phase[32,33]:

$$D_m = \frac{7.4 \times 10^{-8} \sqrt{x_A \phi_A M_A + x_B \phi_B M_B} T}{\eta_{AB} V_b^{0.6}} \quad (4)$$

where x_A and x_B, ϕ_A and ϕ_B, M_A and M_B are the molar fractions, the associative factors (1.9 for methanol, 2.6 for water), and the molecular weights (g/mol) of the two solvents A and B used (32 g/mol for methanol, 18 g/mol for water), respectively, η_{AB} is the viscosity (cP) of the binary eluent listed in,[25] and V_b is the molar volume of the compound considered at its boiling point, estimated from the LeBas group method.[32] Note that independent experimental studies have shown that the values of D_m measured with the Aris-Taylor method using long widely coiled capillary tubes ($\simeq$15 m long, $\simeq$0.5-mm internal diameter) kept at constant temperature differ by less than $\pm$ 10% from the Wilke and Chang estimates.[33]

The parameter δ_0 in Eq. 1 is written as follows:

$$\delta_0 = \frac{1-\varepsilon_e}{\varepsilon_e}[\varepsilon_p + (1-\varepsilon_p)K] \quad (5)$$

where ε_p is the porosity of the solid adsorbent and K is the Henry's constant of the compound considered:

$$K = \frac{\varepsilon_t}{1-\varepsilon_t} k' \quad (6)$$

where $\varepsilon_t = \varepsilon_e + (1-\varepsilon_e)\varepsilon_p$ is the total porosity of the bed and k' is the compound retention factor.

The term $h_{\text{eddy}}(v)$ accounts for the band broadening contribution due to the local flow heterogeneities in the packed bed, at the scale of the particles (transchannel, the short-range interchannel, and the long-range interchannel effects) and at the scale of the column radius (transcolumn effect). Assuming each type of velocity bias to be independent of the others, the overall eddy dispersion term writes as follows:

$$h_{\text{eddy}}(v) = h_{\text{transchannel}}(v) + h_{\text{SR-interchannel}}(v) + h_{\text{LR-interchannel}}(v) + h_{\text{transcolumn}}(v) \quad (7)$$

For each type of flow heterogeneity, a flow and a diffusion exchange mechanisms occur simultaneously, allowing sample molecules to be transferred between different flow streamlines. In general, these two mechanisms are not independent. They are coupled as described in the coupling theory of eddy dispersion by Giddings.[11]

In this work, we combine the pore blocking, the peak parking, and the results of h measurements in order to determine each parameter $D_{\text{eff}}(v=0)$, Ω, $h_{\text{eddy}}(v)$, and k_f in Eq. 1 and compare them when the access to the mesopores is blocked or free.

Calculation of the reduced column HETP

Two different approaches were considered in this work for the acquisition of h data, the method of the moments and the measurement of the half-height peak bandwidth.

Moment analysis

This first method provides a priori the true column HETP by considering the complete distribution of the sample concentration during elution, from $t = 0$ to $t = \infty$. Equal importance is given to all the eluted concentrations from the very base to the apex of the peak. The first moment (μ_1) and the second central moment (μ_2') of the peaks were measured according to:

$$\mu_1 = \frac{\int_0^\infty C(t)t dt}{\int_0^\infty C(t) dt} \quad (8)$$

$$\mu_2' = \frac{\int_0^\infty C(t)(t-\mu_1)^2 dt}{\int_0^\infty C(t) dt} \quad (9)$$

In this work, a finite upper time limit was applied (instead of $t = \infty$) in the numerical integration of the peak profiles.

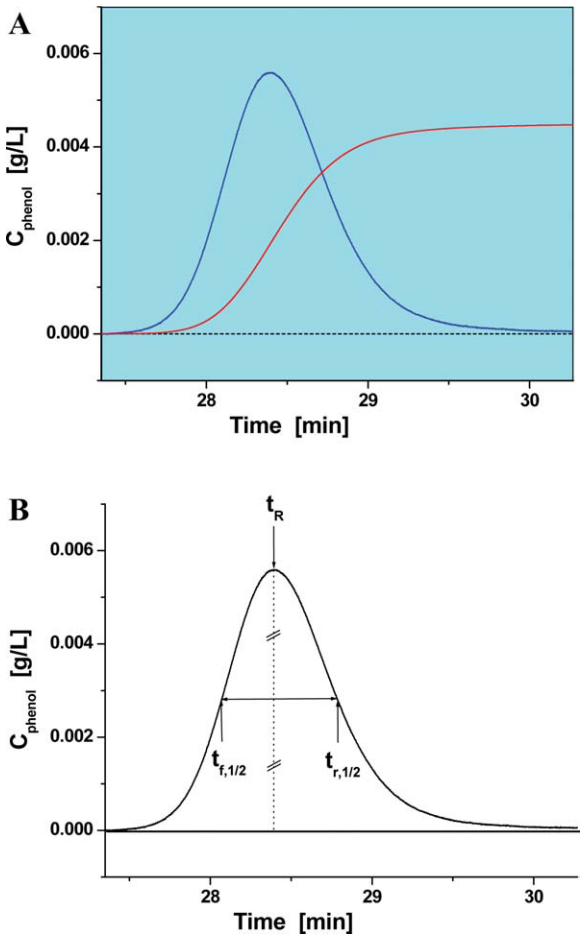

Figure 1. (A) Determination of the *h* data by measuring the first two moments of the concentration distribution represented by the solid black line; the upper integration limit is chosen once 99.5% of the injected mass is eluted as represented by the solid red line or the cumulative eluted mass; (B) determination of the *h* data from the measurement of the elution time at the peak apex (t_R) and the bandwidth at half the height of the peak ($t_{r,1/2} - t_{f,1/2}$).

[Color figure can be viewed in the online issue, which is available at www.interscience.wiley.com.]

This upper limit was unambiguously defined as corresponding to the elution of 99.5% of the sample mass from the column outlet (see the cumulative mass represented by the red curve in the examples given in Figure 1A). The same strategy was applied for the determination of the first ($\mu_{1,ex}$) and the second central ($\mu'_{2,ex}$) moments of the profiles recorded when the chromatographic column was replaced with a zero volume union connector.

The reduced column HETP, h, is determined using the following definition:

$$h = \frac{L}{d_p} \frac{\mu'_2 - \mu'_{2,ex}}{(\mu_1 - \mu_{1,ex})^2} \tag{10}$$

where L is the column length.

Equation 10 provides the maximum expected reduced HETP values, compared with other estimates based on geometrical considerations, such as the Foley-Dorsey equation.[34] In the following section, we consider the simplest geometrical method, which is based on the measurement of only two data per peak, the elution time at the peak apex and its bandwidth at half the height of the peak.

Half-height peak bandwidth method

This second approach consists in measuring the elution time of the peak at its apex and its bandwidth at exactly half its height (see example in Figure 1B). This method ignores the consequences of a possible peak asymmetry due to the tailing and/or the fronting of the peak close to its base. The three corresponding elution times are t_R, $t_{f,1/2}$ (adsorption front), and $t_{r,1/2}$ (desorption rear). The same procedure is respected for the analysis of the extra-column band profiles and the measurement of the elution times $t_{R,ex}$, $t_{f,1/2,ex}$, and $t_{r,1/2,ex}$.

The reduced HETP is given by:

$$h = \frac{L}{d_p} \frac{(t_{r,1/2} - t_{f,1/2})^2 - (t_{r,1/2,ex} - t_{f,1/2,ex})^2}{5.545(t_R - t_{R,ex})^2} \tag{11}$$

Experimental

Chemicals

The mobile phases used in this work were either pure water or a water–methanol mixture (90/10 v/v). Water, methanol, dichloromethane, and *n*-nonane were all purchased from Fisher Scientific (Fair Lawn, NJ) and used without further purification. The mobile phase was filtered before use on a surfactant-free cellulose acetate filter membrane, 0.2 μm pore size (Suwannee, GA). Sodium nitrate, thiourea, and phenol, selected as injected samples, were also from Fisher Scientific.

Materials

The 150 $\times$ 4.6 mm endcapped Luna(2)-C_{18} (100 Å average pore size, 427 m^2/g specific surface area) and Jupiter-C_{18} (320 Å average pore size, 155 m^2/g specific surface area) columns used were gifts from the column manufacturers (Phenomenex, Torrance, CA). The total porosities of the two column beds were measured by pycnometry[35] at 21°C, using methanol (density $\rho_{CH_3OH} = 0.791 \pm 0.001$ g/cm^3) and dichloromethane (density $\rho_{CH_3CN} = 1.326 \pm 0.001$ g/cm^3) as the two eluents. The masses of the Luna(2)-C_{18} column filled with methanol or dichloromethane were 78.94565 and 79.79940 $\pm$ 0.00005 g, respectively, so $\varepsilon_{t,Luna(2)\text{-}C_{18}} = 0.640 \pm 0.003$. The same masses measured with the column Jupiter-C_{18} were 78.68950 and 79.70990 g, so $\varepsilon_{t,Jupiter\text{-}C_{18}} = 0.765$.

The external porosities of the Luna(2)-C_{18} and Jupiter-C_{18} columns ($\varepsilon_e = 0.361$ and 0.387 ± 0.001, respectively) were determined from the results of the total pore-blocking experiments,[36] using sodium nitrate as the unretained compound.

Apparatus

The measurements were made with a HP1090 liquid chromatograph series II (Hewlett-Packard, Palo Alto, CA). This instrument includes a ternary solvent delivery system, an auto-sampler with a 250 μL sample loop, a diode-array UV detector (cell volume 1.7 μL, sampling rate 25 Hz), a column air-oven, and a data station. From the exit of the Rheodyne injection valve to the column inlet and from the column outlet to the detector cell, the total extra-column volume of the instrument is 46 μL, measured as the apparent hold-up volume of a zero-volume union connector in place of the column. The flow-rate delivered by the three pumps was measured at column outlet, under atmospheric pressure. During the HETP measurements, the flow rates were fixed at 0.10, 0.25, 0.50, 0.75, 1.00, 1.75, 2.50, and 3.25 mL/min. The maximum inlet pressure recorded was around 350 bar at 3.25 mL/min for both columns using the aqueous solution of methanol (10%).

The accuracy of the flow rate was checked by collecting in a 25 mL volumetric glass the mass of water pumped through the column during 25 min, at a flow rate set at 1 mL/min, and at 294 K. The mass of water was 24.895 g. The density of pure water at 294 K is $\rho_{H_2O} = 0.9980 \pm 0.0005$ g/cm^3 and the expected mass (25 mL) was 24.950 g, so the flow rate accuracy delivered by the pump is -0.22%.

The laboratory temperature was kept constant at 294 $\pm$ 1K by the laboratory temperature control system.

Parking method experiment

The peak parking method was initially designed to determine the obstruction factor γ_e of columns packed of nonporous particles in gas chromatography.[37] This method was later used to measure the obstruction coefficient of LC columns.[38,39] It is based on the determination of the band broadening caused by longitudinal diffusion along the column when no flow rate is applied. The longitudinal diffusion coefficient $D_{eff}(v = 0)$ contains the contributions of axial diffusion in the interstitial column volume and of diffusivity across the particles when the particles are porous.

A 5 μL diluted sample solution (0.02 g/L) was injected at the desired flow rate (chosen depending on the retention factor, k', of the sample, 0.25 mL/min with thiourea, 1.00 mL/min with phenol). Elution is performed during the time necessary for the band to reach about half the column length. The flow is then abruptly stopped and the sample let free to diffuse along the column bed during a certain parking time t_p. Four different parking times (e.g., 30, 120, 300, and 480 min) were used. Finally, the mobile phase stream is resumed, and the elution profiles are recorded. The slope of a plot of the peak variance μ'_2 vs. the parking time is proportional to the effective axial dispersion coefficient $D_{eff}(v = 0)$ along the column[38]:

$$\frac{\Delta\mu'_2}{\Delta t_p} = \frac{2D_{eff}(v=0)}{u_R^2} \tag{12}$$

where u_R is the linear velocity of the compound band along the column, with

$$u_R = \frac{F_v}{\varepsilon_t \pi r_c^2 (1 + k')} \tag{13}$$

where F_v is the flow rate, r_c the column tube radius (0.23 cm), and k' the retention factor of the sample. Note that when the mesopores of the porous particles are blocked $\varepsilon_t = \varepsilon_e$ ($\varepsilon_p = 0$) and $k' = 0$.

The peak parking method was applied to estimate the effective particle diffusivity D_p by assuming as a first approximation that the contribution of the interstitial and particle volumes to the overall sample diffusion through the packed bed are additive. Accordingly, D_p was calculated from the following equation[38]:

$$D_p = \frac{[\varepsilon_t + (1 - \varepsilon_t)K]D_{eff}(v=0) - \varepsilon_e \gamma_e D_m}{1 - \varepsilon_e} \tag{14}$$

Note that the true value of D_p cannot be known. Equation 14 provides the simplest possible link between D_p and the experimental value of D_{eff}. It assumes the validity of the parallel diffusion model of Knox and Giddings. We want to emphasize that Eq. 14 may provide only a fair estimate of the effective particle diffusivity and that it is, unfortunately, impossible to assess the accuracy of this value of D_p, given the complex structure of the binary composite made of the porous particles and the interstitial eluent. This assessment would require the direct measurement of D_p in the absence of interstitial volume, e.g., by using the sole particles filled with the eluent. A complete different experimental set-up than those used in classical HPLC measurements would be needed.

Pore-blocking experiment

To measure the external porosity of packed or monolithic columns, it is convenient to block the mesopores of the adsorbent and prevent their access to both eluent and probe compounds. This method has the advantage of providing more precise results than the conventional inverse size-exclusion chromatographic experiments but at the cost of the long equilibration time necessary before being able to perform measurements having a relative standard deviation less than 0.2%.[37]

Both Luna-C_{18} and Jupiter-C_{18} columns were initially rinsed with 2-propanol on the HP1090 instrument for 90 min, at a flow rate of 1.0 mL/min, then flushed with nonane for another 90 min by using an auxiliary pump, at a flow rate of 2.0 mL/min. The column is then replaced to the HP1090 instrument, which was first purged with 60 mL of pure water at a flow rate of 4 mL/min to remove all 2-propanol from the instrument. Finally, the nonane present in the interstitial void volume of the column is expelled by flushing the column with a stream of pure water, at 3.50 mL/min, until the baseline of the detector is noiseless, and the first moments of successive injections of dilute NO_3^- are highly reproducible (RSD < 0.2 %). This last step required approximately 200 min or 700 mL of water, which represents nearly 700 interstitial column volumes.

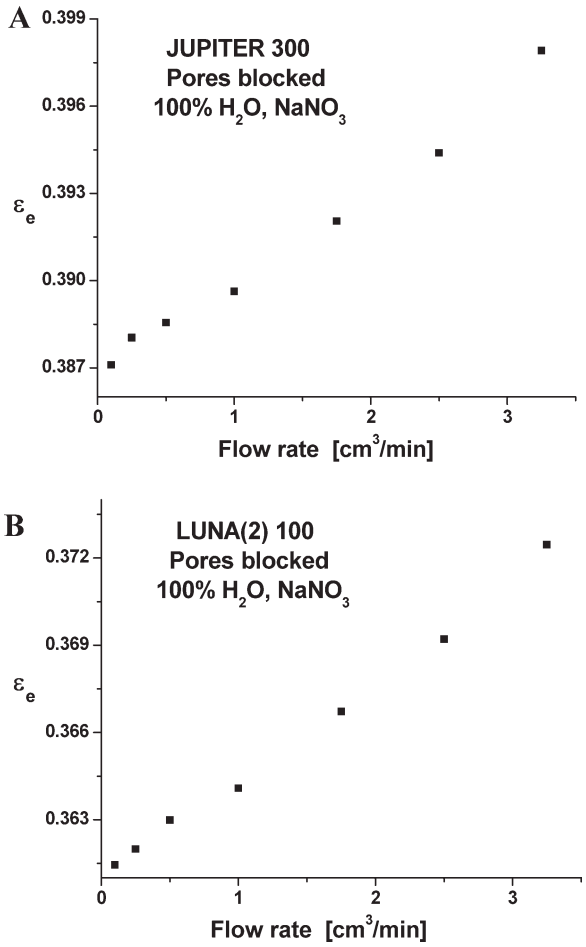

Figure 2. Measurement of the external porosity of the Jupiter-C_{18} (A) and Luna(2)-C_{18} (B) columns after total blocking of the mesopores by *n*-nonane and injection of sodium nitrate in pure water as a function of the fow rate applied.

The decrease of the external porosity as the flow rate decreases is due to expansion of nonane and C_{18} -bonded chains inside the mesopores. The external porosity was extrapolated at a zero flow rate.

Results and Discussion

We discuss first the results of the pore blocking and the peak parking experiments used to measure the external porosities, ε_e, the interstitial obstruction factors, γ_e, of both Jupiter and Luna(2) columns, and the molecular diffusion coefficients, D_m, of thiourea and phenol in the eluents used (water and water–methanol mixture, 90/10, v/v). Second, we analyze the h data measured when the mesopore volume was blocked and when it was not. We compare the eddy dispersion terms, h_{eddy}, and the film mass transfer coefficients, k_f, measured in both cases. Finally, consistent with the observations, we propose a general expression of the trans-column eddy dispersion term, $h_{transcolumn}$, in packed columns.

Determination of the external porosity ε_e of the columns

Figures 2A and B show the corrected and normalized elution volumes of the anion nitrate, $F_v \times \left(\mu_{1,NO_3^-} - \mu_{1,NO_3^-,ex}\right)/V_C$, as a function of the flow rate applied, from 0.10 to 3.25 mL/min. The mesopores of both the Luna(2)-C_{18} and the Jupiter-C_{18} adsorbents were filled by liquid *n*-nonane, according to the protocol given in the experimental section. NO_3^- was eluted with 100% water and detected at 225 nm. Because of its high polarity and strong affinity for water, nitrate anions do not dissolve into *n*-nonane and are completely excluded from the mesopore network of both columns. The porous particles behave as if they were nonporous with respect to the elution of NO_3^-. Figures 2A and B provide the reduced (to the column tube volume V_c) interstitial volume accessible to the nitrate anion. We will assume that this volume is the same for any small molecules, such as thiourea and phenol, which will be used as complementary samples in the next parts of this work.

It is striking to observe that the external porosity of the packed bed apparently increases when the flow rate increases. Had the particles been nonporous because they were solid, this increase in the elution time of the nitrate ion would be explained by the compressibility of the eluent water from atmospheric pressure to the average column pressure measured when a flow rate of 3.25 mL/min was applied ($\sim$200 bar). The compressibility of water being 0.46×10^{-4} bar^{-1},[40] the volume of water pumped under atmospheric pressure to fill the interstitial volume would increase by less than 1.0%. In contrast, the experimental data in Figures 2A and B showed an increase of the relative interstitial volume of $\frac{0.372-0.361}{0.361} = 3.0\%$ and $\frac{0.398-0.387}{0.387} = 2.8\%$ in Luna(2)-C_{18} and Jupiter-C_{18} columns, respectively. This proves that the eluent compresses the liquid *n*-nonane trapped inside the mesopores and the C_{18} -bonded layer.

Combining the results of pycnometry measurements ($\varepsilon_{t,Jupiter\text{-}C_{18}} = 0.765$ and $\varepsilon_{t,Luna(2)\text{-}C_{18}} = 0.640$) and the extrapolated elution volumes of the nitrate anions to a zero column pressure drop ($\varepsilon_{e,Jupiter\text{-}C_{18}} = 0.387$ and $\varepsilon_{e,Luna(2)\text{-}C_{18}} = 0.361$), it is possible to determine the volume of liquid *n*-nonane, V_{nonane}, trapped inside the mesopores of the Jupiter-C_{18} and Luna(2)-C_{18} porous particles per column ($V_{nonane} = (\varepsilon_t - \varepsilon_e)V_C$), e.g. 0.942 cm^3 and 0.696 cm^3, respectively. In addition, the volumes of the C_{18} -bonded layer, $V_{C_{18}}$, in the two columns can be estimated from the density of neat silica (2.20 g/cm^3), the surface coverage in C_{18} chains (5.48 and 3.20%), and the specific surface area of bare silica (155 and 427 m^2/g). Assuming a density of alkyl bonded chains of about 0.80 g/cm^3 and neglecting the volume contributions of the endcapping reagent, the mass of silica in the Jupiter and Luna(2) columns were found equal to 0.783 and 0.968 g, respectively. The volumes of the C_{18} -bonded layer are 0.230 and 0.457 cm^3.

The compressibilities of *n*-nonane and octadecyl chain are close to 1.2×10^{-4} bar^{-1} and 0.8×10^{-4}, respectively.[40] Increasing the average column pressure from 0 to 200 bar, compresses the initial volume of *n*-nonane and C_{18} -bonded chains by $200 \times (0.942 \times 1.210^{-4} + 0.230 \times 0.810^{-4}) = 0.026$ cm^3 in the Jupiter column. The same diminution of volume in the Luna(2) column is 0.024 cm^3. These values represent 2.7% of the interstitial volume measured at zero bar pressure and match nearly the variation of external porosities observed in Figures 2A and B when the flow rate (or the average column pressure) increases from 0 to 3.25 mL/min (or from 0 to 200 bar). This confirms the sensitivity

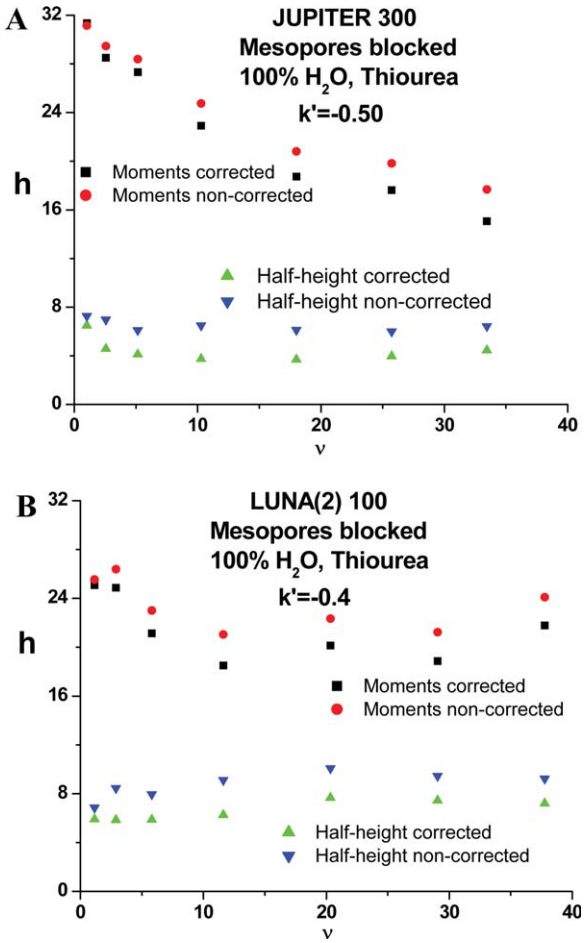

Figure 3. Plot of the reduced HETPs of thiourea after total blocking of the mesopores of the Jupiter-C_{18} (A) and Luna(2)-C_{18} (B) columns with *n*-nonane.

$T = 294$ K. Mobile phase: pure water. The h data are given according to the measurement of the first two moments of the peak (full squares and full circles) and to the measurement of the bandwidth at the peak half-height (full triangles). Note that the reduced HETPs are meaningfull only when the second measurement method is used for the determination of the h data. Note also the high value of the reduced HETP plateau at high linear velocities, 5 with Jupiter and 7 with Luna(2) column. [Color figure can be viewed in the online issue, which is available at www.interscience.wiley.com.]

and the good precision of the pore blocking method. On the other hand, it is difficult to check the accuracy of the method because the exact location of the initial interface between nonane and water at the external surface area of the particles is unknown after *n*-nonane was flushed out of the interstitial volume by a flow of water at 3.5 mL/min during 200 min.

Determination of the obstruction factor γ_e of the columns

The obstruction factors of both columns were measured from the known molecular diffusion coefficient of thiourea in pure water[29,30] at 298 K. It was corrected for the change in temperature and water viscosity from $T = 298$ K to $T = 294$ K. Accordingly, $D_m = 1.21 \times 10^{-5}$ cm^2/s. Note that the Wilke and Chang correlation[31] predicted a value of 1.13×10^{-5} cm^2/s or a relative error of -6.6%. The mesopore volume was blocked by trapping liquid *n*-nonane into them as described previously. The peak parking method was used and the effective diffusion coefficient $D_{eff}(v = 0)$ of thiourea along the packed bed was measured from the analysis of the slope of the peak parking plot, μ'_2 vs. t_p. The flow rate was set at 0.25 mL/min. When the mesopores are blocked, the compound is constrained to diffuse around the packed particles, making the actual diffusion path longer than a direct straight diffusion path. The contributions of tortuosity and constriction are bunched into the obstruction factor γ_e and:

$$D_{eff}(v = 0) = \gamma_e D_m \tag{15}$$

We measured a value of $D_{eff}(v = 0) = 7.30 \times 10^{-6}$ cm^2/s and 7.16×10^{-6} cm^2/s with the Jupiter and the Luna(2) columns, respectively. The corresponding values of the obstruction factors γ_e are 0.605 and 0.594, as expected for a random packing of spherical particles[37,41] with an external porosities around 0.4.

Determination of the diffusion coefficients of thiourea and phenol in methanol/water 10/90

The diffusion coefficient of thiourea in a mixture of methanol and water (90% water in volume) was measured by using the peak parking method (Luna(2)-C_{18} column) and by replacing pure water with the new mobile phase containing 10% of methanol. The solubility of nonane in dilute solutions of methanol in water being very low, the addition of 10% methanol to water does not extract *n*-nonane from the mesopore volume of the columns at the flow rate of 0.25 mL/min (the first moment of thiourea changes by less than 0.2%, from 3.809 to 3.811 min). The effective diffusion coefficient was found to be $D_{eff}(v = 0) = 5.74 \times 10^{-6}$ cm^2/s. Accordingly, the molecular diffusion coefficient of thiourea in methanol/water (10/90 v/v) and at 294 K is equal to 9.67×10^{-6} cm^2/s. The value given by the Wilke and Chang correlation is 8.74×10^{-6} cm^2/s (relative error -10.0%) by considering the new eluent viscosity of the mixture at 1.28 cP (0.98 cP in pure water).[25]

The diffusion coefficient of phenol ($D_m = 8.10 \times 10^{-6}$ cm^2/s) in the same methanol/water mixture was derived from the power 0.6 of the ratio of the molar volumes of the two compounds, thiourea (77 cm^3/mol) and phenol (103.4 cm^3/mol), estimated from the LeBas group contribution method.[32]

Determination of the eddy dispersion term of the columns when the mesopores are blocked

The HETPs of both the Jupiter and Luna(2) columns were measured by blocking the access of thiourea to the mesopore volume. Pure water was used a the eluent. Figures 3A and B show the experimental HETPs measured by the approaches described in the theoretical section. In addition, the HETPs corrected and non-corrected for the extra-column contributions are represented in the same graphs.

First, we observe a large difference in the results depending on the method used to measure the column HETPs. The values obtained with the method of the moments which

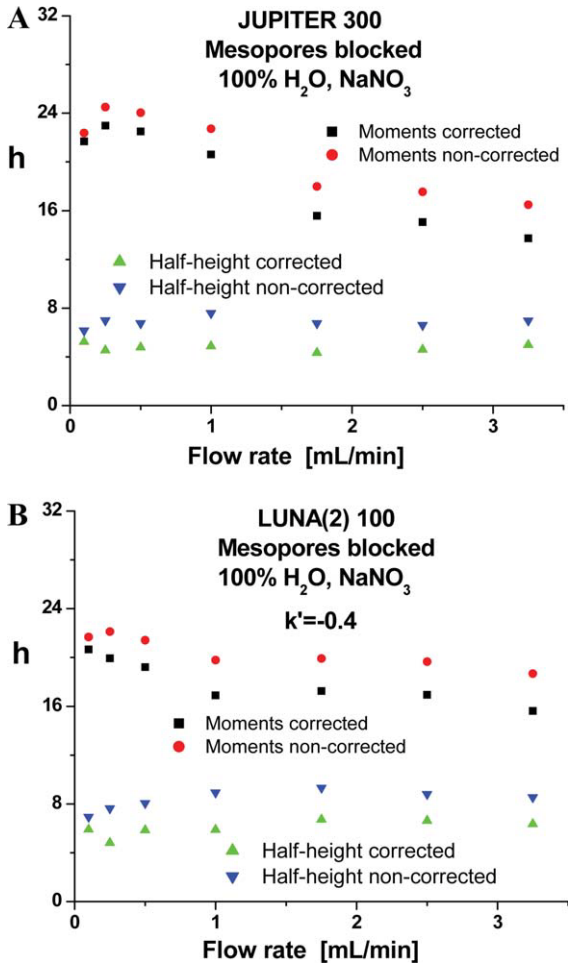

Figure 4. Same as in Figures 3A and B, except the injection of sodium nitrate.

Note the confirmation of the h data measured with thiourea at high reduced linear velocities. $h = 5$ and $h = 7$ on Luna(2) and Jupiter columns, respectively. [Color figure can be viewed in the online issue, which is available at www.interscience.wiley.com.]

consider 99.5 % of the sample mass eluted (starting from the front part of the peak) are about three times larger than those measured from the half-height peak method at the highest reduced linear velocity. This systematic difference is explained by the high sensitivity of the second central moment μ'_2 to band tailing and to the low concentration distribution measured at long elution times, especially when low flow rates are applied. Considering the peak half-height method eliminates this problem and the reduced HETPs remain quasi-constant over the experimental range of linear velocities which seems to make more sense than the decreasing HETP curves obtained when the method of moments is applied. The analysis of the contribution of the concentration distribution on the first four moments of a chromatographic peak is discussed in,[25] which suggests that the method of moments fails to measure meaningful mass transfer data in HPLC columns due to the error made on the measurement of the second central moments. The measurements made in this work confirms this conclusion.

Because the elution volumes of the sample are small when the mesopores are blocked (950 μL), the effect of the extra-column contributions (45 μL or 5% of the hold-up volume) is clearly visible on the plots (error of +2 to 3 reduced HETP unit). The accurate measurement of the eddy dispersion term in packed columns when the sample has no access to the mesopore volume requires due correction for the extra-column contributions.

Interestingly, the reduced eddy dispersion term of Luna(2) column ($h_{eddy} \simeq 7$, half-height bandwidth method) is slightly larger than that of the Jupiter column ($h_{eddy} \simeq 5$) when the access to the mesopore is blocked. This was confirmed by injecting sodium nitrate instead of thiourea as shown in Figures 4A and B. This value is significantly larger than 2, the value predicted by the coupling theory of eddy dispersion of Giddings[11] when only trans-channel, short-range interchannel, and long-range interchannel velocity biases are considered. A contribution related to the trans-column flow heterogeneity has to be added. This will be discussed later, together with the h data measured when access to the mesopore volume of the particles is free.

These data suggest that the packing of highly porous particles (Jupiter-C_{18}, $\varepsilon_p = 0.617$) is more radially homogeneous than that of less porous particles (Luna(2)-C_{18}, $\varepsilon_p = 0.437$).

Determination of the HETP terms of the columns when the mesopores are unblocked for unretained compounds

Liquid n-nonane trapped inside the particle mesopores of the columns was removed by flushing the column with pure 2-propanol at a flow rate of 0.5 mL/min for an hour. The elimination was rapid and shown by the appearance of a noisy UV signal at a wavelength of 252 nm. Thiourea was used as the nonretained compound, eluted with 10% methanol in pure water, to avoid pore dewetting at very low flow rate (i.e,, at low average column pressure). The reduced HETP plots are given in Figure 5A and B.

The HETPs measured with the method of the moments are now only about twice as large as those measured by the peak half-height method, instead of three times when the mesopores were blocked. The contribution of the extra-column volume to the column HETP is smaller because the elution volumes of thiourea are larger, at about 2.0 and 1.70 mL with the Jupiter and Luna(2) columns, respectively. The extra-column volume represents now less than 2.5 % of the sample elution volume and its effect on the band broadening is almost negligible as shown by the small distance between the corrected and noncorrected h data in Figures 5.

The parking experiments (Eq. 12) give $D_{eff}(v = 0) = 7.22 \times 10^{-6}$ and 4.62×10^{-6} cm^2/s for the Jupiter and Luna(2) columns, respectively. The diffusion coefficient of thiourea in methanol/water (10/90 v/v) was found to be 9.67×10^{-6} cm^2/s. Both effective diffusion coefficients are smaller than D_m due to obstruction for diffusion in both large interstitial throughpores and small internal mesopores. Also consistent with the structure of the two columns is the larger effective diffusivity observed for Jupiter-C_{18}, the particles of which have a larger internal volume than those of Luna(2)-C_{18} ($\varepsilon_p = 0.617$ instead of 0.437) and a larger average mesopore size. These characteristics cause a smaller hindrance for

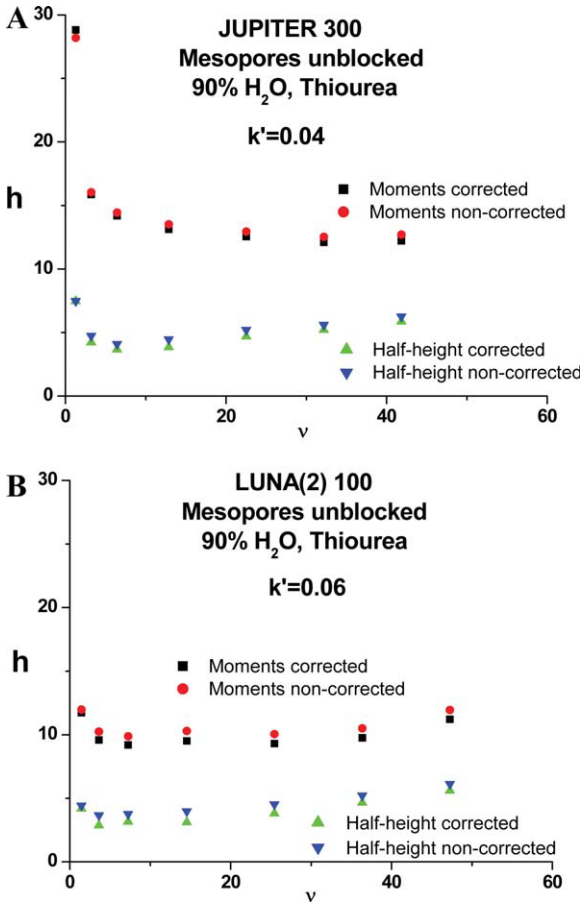

Figure 5. Same as in Figures 3A and B, except the mesopores were unblocked and 10% methanol was added to pure water avoid pore dewetting.

Note the diminution of the extrapolated high velocity A term to $h \simeq 4.5$ on both columns. [Color figure can be viewed in the online issue, which is available at www.interscience.wiley.com.]

sample diffusion through the particles of the former material. The effective particle diffusion coefficients are measured according to Eq. 14 and found to be 5.65×10^{-6} and 1.64×10^{-6} cm^2/s in the Jupiter and Luna(2) columns.

Despite the 3.5 ratio of the effective particle diffusivities of these two packing materials, the experimental reduced HETP showed no significant difference between the overall Cv term of the two columns. This proves that the resistance to mass transfer due to trans-particle diffusion is not responsible for the slope of the Cv term. This can be verified from a theoretical point of view by calculating the C_p term in the general rate model of chromatography for spherical particles.[26] The C_p coefficient is given in Eq. 1, which gives 0.0095 and 0.0241 for the Jupiter and Luna(2) columns, respectively. The measurements were made at a maximum reduced linear velocity of ~40. So, the maximum expected contribution of the trans-particle mass transfer resistance is of the order of 0.4 and 1.0 h unit. But the experimental values of the overall C terms are similar on both columns, close to 0.075. This proves that either the film mass transfer resistance or the $C_f v$ term controls the h data at high reduced velocities.

In the general HETP model, we assumed that the Sherwood number was proportional to $v^{1/3}$:

$$Sh = \frac{k_f d_p}{D_m} = \alpha v^{1/3} \tag{16}$$

The Wilson & Geankoplis correlation[7] predicts an α value of $\frac{1.09}{\varepsilon_e^{2/3}}$ ($\simeq 2.1$ with $\varepsilon_e = 0.38$). The Kataoka correlation gives an α value of $1.85(1 - \varepsilon_e)^{1/3}$ ($\simeq 1.6$ with $\varepsilon_e = 0.38$).[42] However, these two correlations are based on experiments performed with nonporous solid particles and may serve here only as reference.

The h data were fitted to the model Eq. 1 to extract the best values of the A-term and of α. We found reduced A terms of 3.2 and 2.1 on Jupiter and Luna(2) columns, respectively and the same value $\alpha = 0.22$ from the data given by the half-height method.

These results are of paramount importance because they show that (1) the eddy dispersion term of chromatographic columns is much lower for columns packed of porous particles, by a factor of 2.5 and 3.5 for the Jupiter and the Luna(2) columns, respectively, than for columns packed of nonporous particles; and (2) the film mass transfer coefficient k_f is much smaller for the former columns, nearly 90% smaller than for columns packed of nonporous particles, and smaller than predicted by the classical correlations. In the following section, we discuss the values of the eddy dispersion term A and the coefficient α for a strongly retained compound.

Determination of the HETP terms of columns having mesopores accessible to strongly retained compounds

Thiourea was replaced with phenol to measure the column efficiency for a compound with a large retention factor (6.5 for Jupiter and 15.5 for Luna(2) columns). The mobile phase composition remained the same (10% methanol in water, v/v). The HETP plots are shown in Figures 6A and B. The difference in the h values yielded by the two methods of measurements is smaller than for the unretained thiourea [only +50% with Jupiter, +25% with Luna(2)]. Furthermore, the correction for band broadening due to the extra-column volume is negligble. The same h data (within 0.5%) are obtained whether the first and second central moments were corrected or not.

The parking experiments showed that the effective particle diffusion coefficient, D_p, are much larger with retained phenol than with unretained thiourea. The values are 1.87×10^{-5} and 4.95×10^{-5} cm^2/s in the Jupiter-C_{18} and the Luna(2)-C_{18} particles, respectively. In contrast to the results for thiourea, the effective particle diffusion is larger in Luna(2)-C_{18} than in Jupiter-C_{18} particles. This difference cannot be due to the difference of diffusivity in the mesopore volume. Surface diffusion contributes to nearly 83 and 97% of the total solute diffusivity through the porous Jupiter-C_{18} and Luna(2)-C_{18} particles. Accordingly, the mass transfer resistance term ($C_p v$) due to mass transfer of the sample through the porous particles is negligible on both columns. The best reduced eddy dispersion terms were found

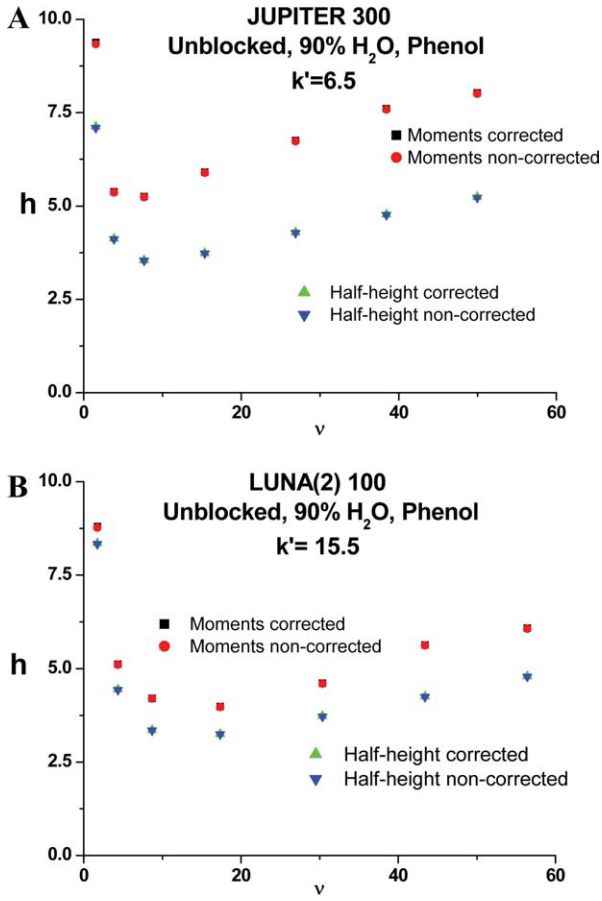

Figure 6. Same as in Figures 3A and B, except the mesopores were unblocked, the injection of phenol, and the addition of 10% methanol to pure water in the mobile phase.

Note the diminution of the extrapolated high velocity A term to $h = 3.5$ (Jupiter) and $h = 2.5$ (Luna(2)). [Color figure can be viewed in the online issue, which is available at www.interscience.wiley.com.]

at 2.5 (Jupiter) and 1.9 (Luna(2)), values slightly smaller than those measured for unretained thiourea (3.2 and 2.1).

There is one plausible explanation for this observation that will be discussed in detail in the following section. The residence time of the sample in the column during its elution considerably decreases when the access to the internal mesopores is blocked. Radial heterogeneity of the packed bed causes trans-column flow heterogeneity, itself leading to the formation of radial concentration gradients. Such gradients are less efficiently relaxed in beds of nonporous particles because the sample cannot laterally diffuse during a sufficiently long time across the column diameter.

The values of the α coefficients are 1.09 (Jupiter) and 0.98 (Luna(2)). k_f is nearly half the value predicted by the Wilson & Geankoplis and the Kataoka correlations. These values are significantly larger than those measured for thiourea. The most likely explanation is that the local concentration gradients taking place between the interstitial mobile phase and the stagnant internal bulk liquid phase at the external surface area of the particles increase with increasing retention. The disagreement between values given by the available correlations and experimental values originates probably from the fact that these correlations were derived from experiments carried out with nonporous particles. Inevitably, the film mass transfer coefficients k_f found with nonporous particles are larger because they ignore the fact that a fraction of the external surface area is liquid. No adsorption and sample uptake takes place at the liquid–liquid interface (moving eluent/stagnant eluent).

Transcolumn eddy dispersion

Measurements of the trans-column (or radial) flow velocity profile have shown it to be close to a fourth degree parabola [$u_0 = u_{0,c} - (r - R_c)^4(u_{0,w} - u_{0,c})$], with $u_{0,c}$ and $u_{0,w}$ the mobile phase velocity in the center of the column and along its wall, respectively, r radial coordinate, and R_c column radius).[18,21,43,44] In good packed columns, the linear velocity is slightly higher in the center than at the column wall (~3–7%). In monolithic columns, the opposite is true.[21] The migration linear velocity, $u_R(x)$, at the reduced radial position x is then:

$$u_R(x) = \frac{\varepsilon_e u(x)}{\varepsilon_t(1+k')} = \frac{\varepsilon_e}{\varepsilon_t(1+k')} u(0)\left[1 - \omega_{\beta,c} x^2\right] \qquad (17)$$

where $\omega_{\beta,c}$ measures the relative amplitude of the parabolic flow profile from the wall ($x = 1$) to the center ($x = 0$) of the column. $u(0)$ is the interstitial linear velocity of the sample in the center of the column. This flow heterogeneity across the column diameter generates radial concentration gradients which are eventually relaxed by radial dispersion. The radial dispersion coefficient $D_r(x)$ in a packed bed is usually written as the sum of two independent contributions, a molecular diffusion one through the whole packed bed volume (interstitial volume + particle volume), D_0, and an eddy dispersion one, $D_{eddy}(x)$, which depends on the reduced radial position $x = \frac{r}{R}$.[41,45] As a first approximation, we may assume that the molecular diffusion coefficient D_0 is equal to the effective axial diffusion coefficient $D_{eff}(v = 0)$ since, when the flow rate is set to zero, packed beds can be considered as isotropic and there is no eddy dispersion:

$$D_r(x) = D_0 + D_{eddy}(x) = \frac{\varepsilon_e \gamma_e + (1-\varepsilon_e)\Omega}{\varepsilon_t(1+k')} D_m + \gamma_r \frac{1}{2} \varepsilon_e u(x)\, d_p \qquad (18)$$

In this equation, $u(x)$ is the interstitial linear velocity at the reduced radial position x. According to precise NMR experiments, the constant γ_r is close to 0.30 for packed beds.[41]

Nonporous particles or blocked mesopores: Flow-controlled mechanism

When access to the mesopores is blocked by *n*-nonane, and the column is eluted with pure water, neither thiourea nor sodium nitrate can diffuse through the particles and $\Omega = 0$. They diffuse only across the intersticial space. At the largest flow rate ($F_v = 3.25$ mL/min), the reduced A-term has reached its constant value on both columns. The residence time t_R of the sample is of the order of 20 sec. The average radial dispersion coefficient being $D_r = 2.72 \times 10^{-5}$ cm^2/s,

the average radial distance from its entrance location to which a thiourea molecule could move within this time is $\sqrt{2D_r t_R} = 0.033$ cm. The column radius is 0.23 cm, which means that thiourea molecules entering in the column center may access only 15% of the distance separating the center and the wall of the column. Undoubtedly, radial band dispersion is mostly controlled by a flow mechanism. The reduced eddy HETP term associated with the flow profile Eq. 17 is: (Gritti F, Guiochon G. New insights on mass transfer kinetics in chromatography submitted)

$$h_{\text{transcolumn}} = \frac{L}{d_p} \frac{\frac{\omega_{c,\beta}^2}{1-\omega_{c,\beta}} - \ln^2(1-\omega_{c,\beta})}{\ln^2(1-\omega_{c,\beta})} \tag{19}$$

The HETP of the column is obtained by adding this trans-column term to the eddy dispersion terms originating from trans-channel, short-range inter-channel, and long-range inter-channel velocity biases as thoroughly discussed by Giddings in his coupling theory of eddy dispersion.[11] The sum of these three HETP contributions is usually of the order of two particle diameters, according to the guesses made by Giddings.[11] Because the reduced HETPs of the Jupiter and Luna(2) columns measured at high reduced linear velocities are 5.0 and 7.0, respectively, Eq. 19 must account for the residual. Calculation showed that the relative amplitude of the equivalent parabolic velocity gradient, $\omega_{\beta,c}$, is 3.4 and 4.4% in the Jupiter and the Luna(2) columns, respectively. These values are large because the residence time required to relax the radial concentration gradients ($\simeq$30 min) is much larger than the actual residence time of the sample in the column (20 sec).

Porous particles or unblocked mesopores: Diffusion-controlled mechanism

When the mesopores of either column are accessible, and phenol is the sample, we can reasonably assume that the same interstitial flow profile, $u(x)$, applies. Whether the particles are porous or not, there is no significant flow through the mesopores of the particles. So, $\omega_{\beta,c} = 0.034$ (Jupiter) or 0.044 [Luna(2)]. At a flow rate $F_v = 0.50$ mL/min for which the reduced HETPs are minimum, the residence times are 1700 and 3100 sec on the Jupiter and Luna(2) columns. The average radial dispersion coefficients are 6.23×10^{-6} and 6.91×10^{-6} cm^2/s, respectively. The corresponding radial dispersion lengths are then 0.146 and 0.207 cm which are now of the same order of magnitude as the column internal radius. We need a model of band dispersion that takes into account the radial dispersion of the sample because flow profile alone does not control band dispersion along the column. The general dispersion model of Aris[46] would apply if the following condition is fulfilled:

$$t_R \gg \frac{d_c^2}{\overline{D}_r} \tag{20}$$

This condition means that the residence time of the sample is significantly larger than the radial diffusion time, which is required to cross the column diameter d_c. In the experiments reported in this work, we are in an intermediate situation where both times are comparable. Still, it is possible to estimate the additional reduced HETP term under the asymptotic Aris condition[6]:

$$h_{\text{transcolumn}} = C_m \frac{d_c^2}{d_p \overline{D}_r} u_R = C_m \frac{\varepsilon_e}{\varepsilon_t} \frac{d_c^2}{d_p^2} \frac{D_m}{\overline{D}_r} \frac{1}{1+k'} v \tag{21}$$

where C_m is a constant that is derived from the radial velocity profile, $u(x)$, as follows[7]:

$$C_m \frac{D_0}{\overline{D}_r} = A_0 \tag{22}$$

with

$$A_0 = \frac{I_1 - 2I_2 + I_3}{2} \tag{23}$$

and

$$I_1 = \int_0^1 \frac{\Phi^2(x)}{2x\Psi(x)} dx \tag{24}$$

$$I_2 = \int_0^1 \frac{x\Phi(x)}{2\Psi(x)} dx \tag{25}$$

$$I_3 = \int_0^1 \frac{x^3}{2\Psi(x)} dx \tag{26}$$

with

$$\text{with} \quad \Phi(x) = \int_0^x 2x'\phi(x')dx' \tag{27}$$

In these equations, x' is a dummy variable. The functions $\phi(x)$ and $\Psi(x)$ are the dimensionless radial profiles of the linear migration velocity u and the radial diffusion coefficient D_r, respectively.[45,46] In the particular case discussed here:

$$\phi(x) = \frac{u_R(x)}{u_R} = \frac{u_R(x)}{2\int_0^1 u_R(x')x'dx'} \tag{28}$$

and

$$\Psi(x) = \frac{D_r(x)}{D_0} \tag{29}$$

The calculation of the coefficient C_m gives 4.77×10^{-6} and 7.34×10^{-6} for the Jupiter and the Luna(2) columns. The additional reduced HETP terms are now 1.20 and 0.94 on the Jupiter and Luna(2) columns, respectively, corresponding to total reduced eddy dispersion terms of $2 + 1.20 = 3.20$ and $2 + 0.94 = 2.94$. The calculated contributions of the film mass transfer term with a Sherwood number $Sh = \alpha v^{1/3}$ ($\alpha = 1.09$ and 0.98 for the Jupiter and Luna(2) columns, respectively) are 0.66 and 0.76. The trans-particle mass transfer resistance term is negligible (<0.1). The longitudinal diffusion terms are equal to 0.16 and 0.14. Accordingly, the theoretical HETPs are 4.02 and 3.84, respectively. The experimental HETPs given in Figures 6A and B are slightly smaller, at 3.52 and 3.31, respectively, which is consistent with the fact that the Aris model overestimates the true trans-column effect Because the condition Eq. 20 is not fully satisfied. Actually, the diffusion and flow mechanisms are coupled, as suggested by Giddings 50 years ago.[10]

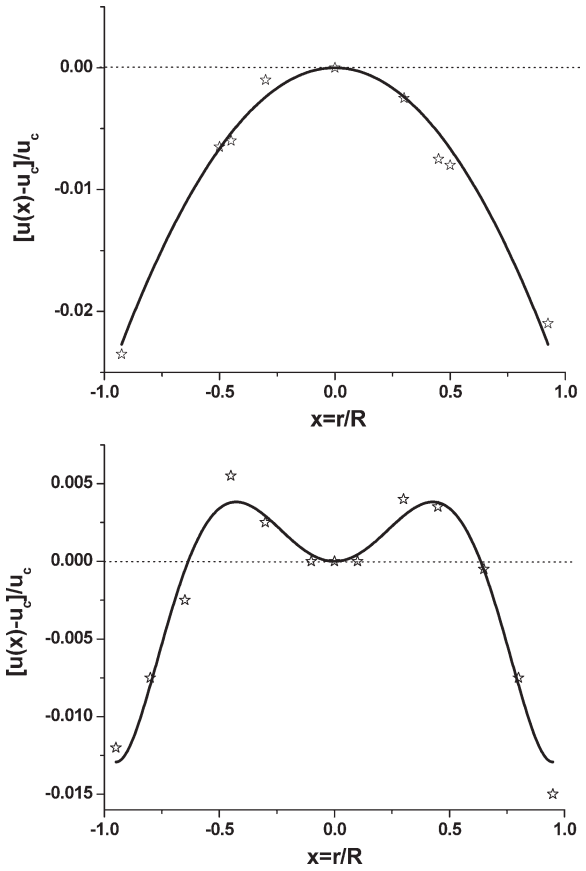

Figure 7. Examples of actual flow profile distributions across the column diameter of packed columns.

(A) 7.8 × 300 mm Zorbax PRO-10/150 packed with spherical 10 μm C_{18} -bonded silica particles. The data were reproduced from Figure 2 of Ref. 44 The profile was fitted to the quartic polynomial given by Eq. 36 (thick solid line). (B) 9.4 mm × 250 mm Zorbax column packed with 5 μm spherical silica-C_8particles (empty stars). The data were reproduced from Figure 8 of Ref.44 The profile was fitted to the sixth degree polynomial in the reduced radial coordinate as x given by Eq. 38 (thick solid line).

In conclusion, there is a very good agreement between prediction and experiment if we consider that flow and diffusion mechanisms are coupled in the expression of the trans-column eddy term. The Aris model accounts well for the decrease of the minimum HETP when the mesopores of the porous particles are unblocked and the residence time in the column increases. When mesopores are blocked, we measured a total reduced eddy dispersion terms of 5.0 (vs. 3.2) and 7.0 (vs. 2.9) on the Jupiter and Luna(2) columns, respectively. This proves that the importance of eddy dispersion depends on whether the mesopore volume is accessible or not to the sample, e.g. if it is rapidly eluted or not. This observation was already reported but had not yet been clearly justified from a fundamental point of view. (Gritti F, Guiochon G. New insights on mass transfer kinetics in chromatography submitted)

Nevertheless, the results reported in Figures 3, 5, and 6 remain surprising. Their fundamental explanation is (1) the flow pattern across a column is heterogeneous; and (2) relaxation of the radial concentration gradients is more effective when beds are packed of porous particles because the residence time inside the column and the radial dispersion coefficient increase.

General expression for the transcolumn eddy dispersion term

Neither the flow mechanism (Eq. 19) nor the diffusion mechanism (Eq. 21) alone control the trans-column eddy dispersion term in packed beds. The understanding of both is necessary to predict this term. Giddings had to couple both mechanisms to derive a physically realistic model of eddy dispersion that is valid in a wide range of reduced linear velocities. For each type of the velocity biases (trans-channel, short-range inter-channel, long-range inter-channel, trans-column), that he identified, Giddings derived two reduced eddy dispersion terms, one when this bias is controlled by a diffusion transfer mechanism, the other when by a flow transfer mechanism[11]:

$$h_{\text{diffusion,i}} = \omega_{\text{i}} v \tag{30}$$

$$h_{\text{flow,i}} = 2\lambda_{\text{i}} \tag{31}$$

In his coupling theory of eddy dispersion, Giddings demonstrated that the actual eddy dispersion term, $h_{\text{eddy,i}}$, is given by a combination of $h_{\text{diffusion,i}}$ and $h_{\text{flow,i}}$:

$$h_{\text{eddy,i}} = \frac{1}{\frac{1}{h_{\text{flow,i}}} + \frac{1}{h_{\text{diffusion,i}}}} = \frac{1}{\frac{1}{2\lambda_{\text{i}}} + \frac{1}{\omega_{\text{i}} v}} \tag{32}$$

If we consider a flow profile given by a parabolic equation, the expression of $h_{\text{diffusion,transcolumn}}$ and $h_{\text{flow,transcolumn}}$ are as follows:

$$h_{\text{diffusion,t}} = C_{\text{m}} \frac{\varepsilon_{\text{e}}}{\varepsilon_{\text{t}}} \frac{d_{\text{c}}^2}{d_{\text{p}}^2} \frac{1}{1+k'} \frac{1}{\Omega_{\text{c}}} v \tag{33}$$

$$h_{\text{flow,t}} = \frac{L}{d_{\text{p}}} \frac{\frac{\omega_{\beta,\text{c}}^2}{1-\omega_{\beta,\text{c}}} - \ln^2(1-\omega_{\beta,\text{c}})}{\ln^2(1-\omega_{\beta,\text{c}})} \simeq \frac{1}{12} \frac{L}{d_{\text{p}}} \omega_{\beta,\text{c}}^2 \tag{34}$$

Introducing Eqs. 33 and 34 into the general equation Eq. 32, we obtain a general expression of the trans-column eddy dispersion term for a packed column:

$$h_{\text{eddy,t}} = \frac{1}{\frac{d_{\text{p}}}{L} \frac{\ln^2(1-\omega_{\beta,\text{c}})}{\frac{\omega_{\beta,\text{c}}^2}{1-\omega_{\beta,\text{c}}} - \ln^2(1-\omega_{\beta,\text{c}})} + \frac{\varepsilon_{\text{t}} d_{\text{p}}^2 (1+k') \Omega_{\text{c}}}{C_{\text{m}} \varepsilon_{\text{e}} d_{\text{c}}^2 v}} \tag{35}$$

The simulation of band broadening originating from various shapes of axisymmetrical trans-column velocity gradients clearly supports the theoretical expression of the trans-column reduced plate height given by Eq. 32.[47] In actual packed columns,[44] the radial flow velocity profiles are better described by a two-term quartic equation or even by a more complex function, as shown in Figures 7A and B. In Figure 7A, the column is the 7.8 × 300 mm Zorbax PRO-

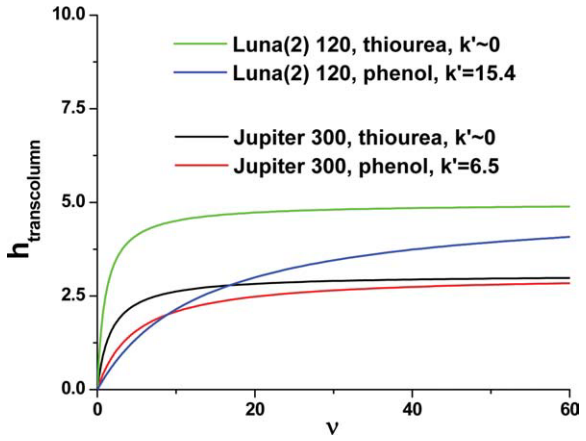

Figure 8. Plot of the transcolumn eddy dispersion term $h_{transcolumn}$ of Jupiter and Luna(2) columns vs. the reduced linear velocity ν and for different retentive condition.

The Giddings' model Eq. 35 is based on the coupling of the flow model Eq. 19 and the diffusion Aris dispersion model Eq. 21. Note the smoother increase of the transcolumn eddy HETP term when the retention factor of the sample increases, e.g when its residence time inside the column is longer. [Color figure can be viewed in the online issue, which is available at www.interscience.wiley.com.]

10/150 packed with spherical 10 μm C_{18}-bonded silica particles.8 The quartic flow profile fits well the local experimental linear velocities:

$$u(x) = u(0)\left[1 - \omega_{\beta,c}x^4\right] \tag{36}$$

where $a = 0.02667$ is the optimized model parameter which gives the smallest residual between the experimental and the model flow velocity profiles. The flow trans-column reduced HETP, $h_{flow,t}$, can be analytically written for $a > 0$:

$$h_{flow,t} = \frac{L}{d_p}\frac{\frac{2\omega_{\beta,c}-(1-\omega_{\beta,c})\sqrt{\omega_{\beta,c}}\ln\left(\frac{1-\sqrt{\omega_{\beta,c}}}{1+\sqrt{\omega_{\beta,c}}}\right)}{1-\omega_{\beta,c}} - \ln^2\left(\frac{1-\sqrt{\omega_{\beta,c}}}{1+\sqrt{\omega_{\beta,c}}}\right)}{\ln^2\left(\frac{1-\sqrt{\omega_{\beta,c}}}{1+\sqrt{\omega_{\beta,c}}}\right)} \simeq \frac{4}{45}\frac{L}{d_p}\omega_{\beta,c}^2 \tag{37}$$

In Figure 7B, the column is a 9.4 mm $\times$ 250 mm Zorbax column packed with 5 μm spherical C_8 -silica particles.[44] We observe a local maximum linear velocity at an intermediate reduced radial position $x = 0.40$. This experimental velocity profile was well fitted to the following sixth order polynomial:

$$u(x) = u(0)\left[1 + ax^2 + bx^4 + cx^6\right] \tag{38}$$

where $a = 0.04493$, $b = -0.14818$, and $c = 0.09146$ are adjustable parameters which minimize the distance between the experimental and the sixth degree polynomial flow profiles. In this specific case, the flow trans-column reduced HETP, $h_{flow,t}$, is derived numerically.

In Eq. 33, Ω_c is the ratio of the column dispersion coefficient at zero linear velocity (diffusion mechanism) to the bulk diffusivity. It is directly estimated from the results of the peak parking experiments.[38,39] $\omega_{\beta,c}$ is derived from the results of the pore blocking experiments and the corresponding h data obtained at high linear velocity (flow mechanism). (Gritti F, Guiochon G. New insights on mass transfer kinetics in chromatography submitted) C_m is a constant which depends only on the radial distribution of the axial flow velocity $u(x)$. The radial profile of the linear flow velocity is conveniently derived from measurements of the radial distribution of the local elution times of an unretained compound, using an in situ electrochemical detection at the column outlet.[42]

Figure 8 shows the variations of the trans-column eddy dispersion terms of thiourea and phenol as functions of the reduced linear velocity in the Jupiter and Luna(2) columns. It illustrates well the fact that the minimum HETP of these columns decreases with increasing retention. The transcolumn eddy dispersion term is smaller with phenol than with thiourea on both columns. It increases steeply for nonretained compounds in the range $0 < \nu < 5$, which explains why the longitudinal diffusion and the eddy dispersion terms compensate each other in Figure 5B (thiourea, Luna(2) column). The h data are nearly constant in the range $0 < \nu < 15$. In contrast, the diffusion branch is clearly visible with phenol in Figure 6B because the trans-column eddy term increases but it does so smoothly. Note that the B term is larger with thiourea, $D_{eff}(\nu = 0) = 4.62 \times 10^{-6}$ cm^2/s than with phenol, 3.17×10^{-6} cm^2/s, which proves that the phenomenon discussed here cannot be due to a difference in the longitudinal diffusion terms.

Conclusion

The eddy dispersion terms of columns having packed beds of identical structure could be very different, depending on whether the mesopore volume of the particles is accessible or not or whether these particles are porous or not. When the mesopores of the Jupiter (300Å) and the Luna(2) (100Å) columns were blocked by liquid n-nonane, their minimum reduced HETPs for thiourea in pure water were 4.5 and 7.0, respectively. In contrast, after removing n-nonane from the mesopores and deblocking their access for the samples, these minimum HETPs dropped to 3.5 and 3.2, respectively, whereas for phenol the minimum HETPs were lower. This significant increase in the column efficiency is explained by a combination of the consequences of the radial heterogeneity of the distribution of mobile phase velocities across the column; and of the importance of surface diffusion that enhances the rate of mass transfer across the particles. We successfully applied the coupling theory of eddy dispersion of Giddings to account for these effects.

Because of the stress and strains that take place in the bed of particles during the slurry packing process of the particles and the eventual consolidation of the bed, the radial distribution of the mobile phase velocities across a packed column is never rigorously flat from the center to the wall of the column but it is heterogeneous. This causes the sample zone to warp during its elution, its central region moving faster than its wall region and significant concentration gradients to build up. Because the detector measures the average concentration across the bulk solution exiting the column, the band

appears to be broadened. When the mesopores are blocked, these gradients may be relaxed only by diffusion from streamlets to streamlets, around particles. In contrast, when the mesopores are accessible, pore diffusion, i.e., diffusion across particles, may contribute to relax these gradients. The diffusion flux across a particle is the sum of the contributions of bulk diffusion or diffusion through the mobile phase contained in the pores of the particle and of surface diffusion or diffusion along the adsorbent surface.[28] The later increases rapidly with increasing concentration gradient along this surface, hence the diffusion flux increases rapidly with increasing retention of the probe compound. The radial concentration gradients due to the heterogeneity of the flow pattern are better relaxed when access of solutes to the pores is free and when these solutes are retained. These predictions were experimentally confirmed on both the Jupiter-C_{18} and Luna(2)-C_{18} columns.

This work suggests that more attention should be paid to the radial profile of the flow velocities across packed columns, as a critical factor for a satisfactory understanding of mass transfer mechanism in RPLC and for the achievement of highly efficient columns. Our work demonstrated that trans-column velocity biases contribute as much as trans-channel, short-range inter-channel, and long-range inter-channel velocity biases all together combined. It also explains why column efficiency depends on the retention of the compound. In theory, the more a column is radially heterogeneous, the more its HETP should decrease with increasing retention factor of the probe used to measure it.

Acknowledgments

This work was supported in part by grant CHE-06-08659 of the National Science Foundation and by the cooperative agreement between the University of Tennessee and the Oak Ridge National Laboratory.

Notation

A_0 = scalar given by Eq. 22
$C(t)$ = sample mobile phase concentration eluted at the column outlet at the time t (kg/m^3)
C_m = Aris's coefficient in Eq. 22
C_f = film solid–liquid mass transfer coefficient
C_p = transparticle solid–liquid mass transfer coefficient
D_0 = radial diffusion coefficient at zero flow rate (m^2/s)
$D_{eddy}(x)$ = additionnal radial diffusion coefficient due to convection at radial coordinate x (m^2/s)
$D_{eff}(v = 0)$ = axial diffusion coefficient in the whole column at zero flow rate (m^2/s)
$\overline{D}_r(v)$ = average radial diffusion coefficient (m^2/s)
d_c = column inner diameter (m)
d_p = average particle size (m)
D_p = particle diffusivity (m^2/s)
D_m = bulk molecular diffusion coefficient (m^2/s)
F_v = flow rate (m^3/s)
h = total reduced column HETP
h_{eddy} = reduced eddy dispersion HETP
$h_{diffusion,i}$ = reduced eddy dispersion HETP of a velocity bias of type i controlled by a diffusion mechanism
$h_{flow,i}$ = reduced eddy dispersion HETP of a velocity bias of type i controlled by a flow mechanism
$h_{transchannel}$ = reduced eddy dispersion HETP due to transchannel velocity biases
$h_{SR\text{-}interchannel}$ = reduced eddy dispersion HETP due to short-range interchannel velocity biases
$h_{LR\text{-}interchannel}$ = reduced eddy dispersion HETP due to long-range interchannel velocity biases
$h_{transcolumn}$ = reduced eddy dispersion HETP due to transcolumn velocity biases
I_1 = scalar given by integral Eq. 24
I_2 = scalar given by integral Eq. 25
I_3 = scalar given by integral Eq. 26
k = retention factor
K = Henry's constant
k_f = film mass transfer coefficient (m/s)
L = column length (m)
M = molecular weight (g/mol)
r_c = internal column tube radius (m)
Sh = Sherwood number
t = elution time (s)
t_p = parking time (s)
t_R = elution time at the apex of the peak (s)
$t_{f,1/2}$ = elution time of the adsorption part of the peak at its half-height (s)
$t_{r,1/2}$ = elution time of the desorption part of the peak at its half-height (s)
$t_{R,ex}$ = elution time at the apex of the extra-column peak (s)
$t_{f,1/2,ex}$ = elution time of the adsorption part of the extra-column peak at its half-height (s)
$t_{r,1/2,ex}$ = elution time of the desorption part of the extra-column peak at its half-height (s)
T = temperature (K)
u = interstitial linear velocity (m/s)
$u(0)$ = interstitial linear velocity at the column center (m/s)
$u_R(x)$ = sample migration linear velocity at the radial coordinate x (m/s)
u_R = average sample migration linear velocity (m/s)
V_b = molar volume of the sample at its boiling point (m^3/mol)
x = reduced radial coordinate
x' = dummy variable in integral Eq. 27
x_A = molar fraction of liquid A in the eluent
x_B = molar fraction of liquid B in the eluent

Greek letters

α = adjustable parameter in Eq. 16
η_{AB} = eluent's viscosity (Pa. s)
δ_0 = retention parameter defined in Eq. 5
ε_e = external column porosity
ε_p = particle porosity
ε_t = total column porosity
ϕ_A = associative factor of liquid A in the eluent
ϕ_B = associative factor of liquid B in the eluent
$\phi(x)$ = dimensionless sample migration linear velocity at the radial coordinate x
$\Phi(x)$ = function given by the integral Eq. 27
$\Psi(x)$ = dimensionless radial diffusion coefficient at the radial coordinate x
γ_e = external obstructive factor with nonporous particles
γ_r = radial obstruction coefficient in Eq. 18
λ_i = flow eddy dispersion coefficient defined in Eq. 30
μ_1 = first moment (s)
$\mu_{1,ex}$ = first moment of the extra-column band profiles (s)
μ'_2 = second central moment (s^2)
$\mu'_{2,ex}$ = second central moment of the extra-column band profiles (s^2)
v = reduced interstitial linear velocity
ω_i = diffusion eddy dispersion coefficient defined in Eq. 30
$\omega_{\beta,c}$ = transcolumn relative velocity inequality for a parabolic flow pattern
Ω = ratio of the particle diffusivity to the bulk diffusion coefficient
Ω_c = ratio of the column diffusivity at zero flow rate to the bulk diffusion coefficient

Literature Cited

1. Miyabe K, Takeuchi S. Surface diffusion of alkylbenzenes on octadecylsilyl-silica gel. *Ind Eng Chem Res.* 1998;37:1154–1158.

2. Gritti F, Guiochon G. Mass transfer equation for proteins in very high-pressure liquid chromatography. *Anal Chem.* 2009;81:2723–2736.
3. Lin HJ, Horváth C. Viscous dissipation in packed beds. *Chem Eng Sci*. 1981;36:47–55.
4. Poppe H, Kraak JC, Huber JFK, Van Den Berg JHM. Temperature gradients in HPLC columns due to viscous heat dissipation. *Chromatographia*. 1981;14:515–523.
5. Gritti F, Guiochon G. Optimization of the thermal environment of columns packed with very fine particles. *J Chromatogr A*. 2009;1216:1353–1362.
6. Gritti F, Martin M, Guiochon G. The influence of viscous friction heating on the efficiency of columns operated under very high pressures. *Anal Chem.* 2009;81:3365–3384.
7. Wilson EJ, Geankoplis CJ. Liquid mass transfer at very low reynolds number in packed beds. *J Ind Eng Chem (Fundam)*. 1966;5:9–14.
8. Miyabe K, Ando M, Ando N, Guiochon G. External mass transfer in high performance liquid chromatography systems. *J Chromatogr A*. 2008;1210:60–67.
9. Giddings JC. Theoretical basis for a continuous, large-capacity gas chromatographic apparatus. *Anal Chem.* 1962;34:37–39.
10. Giddings JC. Evidence on the nature of eddy diffusion in gas chromatography from inert (nonsorbing) column data. *Anal Chem.* 1963;35:1337–1341.
11. Giddings JC. *Dynamics of Chromatography*. Marcel Dekker: New York, NY, 1965.
12. Giddings JC. *Unified Separation Science*. New York, NY: Wiley, 1991.
13. Knox JH. Band dispersion in chromatography—a new view of a-term dispersion. *J Chromatogr A*. 1999;831:3–15.
14. Knox JH. Band dispersion in chromatography—a universal expression for the contribution from the mobile zone. *J Chromatogr A*. 2002;960:7–18.
15. De Ligny CL. The contribution of eddy diffusion and of the macroscopic mobile phase velocity profile to plate height in chromatography: A literature investigation. *J. Chromatogr A*. 1970;49:393–401.
16. Berdichevsky AL, Neue U. Nature of the eddy dispersion in packed beds. *J. Chromatogr A*. 1990;535:189–198.
17. Farkas T, Sepaniak MJ, Guiochon G. Radial distribution of the flow velocity, efficiency and concentration in a wide HPLC column. *AIChE J*. 1997;43:1964–1974.
18. Abia JA, Mriziq KS, Guiochon G. Radial heterogeneity of some analytical-type columns for high performance liquid chromatography. *J Chromatogr A*. 2009;1216:3185–3191.
19. Leinweber FC, Tallarek U. Chromatographic performance of monolithic and particulate stationary phases: hydrodynamics and adsorption capacity. *J Chromatogr A*. 2003;1006:207–226.
20. Kobayashi H, Tokuda D, Ishimaru J, Ikegami T, Miyabe K, Tanaka N. Faster axial band dispersion in a monolithic silica column than in a particle-packed column. *J Chromatogr A*. 2006;1109:2–9.
21. Mriziq KS, Abia JA, Lee Y, Guiochon G. Structural radial heterogeneity of a silica-based wide-bore monolithic column. *J Chromatogr A*. 2008;1193:97–103.
22. Magnico P, Martin M. Dispersion in the interstitial spaces of packed columns. *J Chromatogr A*. 1990;517:31–49.
23. Gritti F, Guiochon G. General HETP equation for the study of mass transfer mechanisms in RPLC. *Anal Chem.* 2006;78:5329–5347.
24. Rhee HK, Aris R, Amundson NR. *First-Order Partial Differential Equations–II. Theory and Application of Hyperbolic Systems of Quasilinear Equations*. Englewood Cliffs, NJ: Prentice–Hall. 1989.
25. Guiochon G, Felinger A, Katti A, Shirazi D. *Fundamentals of Preparative and Nonlinear Chromatography*, *2nd ed*., Academic Press; Boston, MA, 2006.
26. Kucera E. Contribution to the theory of chromatography. linear non-equilibrium elution chromatography. *J Chromatogr A*. 1965;19:237–258.
27. Kubin M. Beitrag zur theorie der chromatographie. 2. einfluss der diffusion ausserhalb und der adsorption innerhalb des sorbens-korns. *Coll Czech Chem Commun*. 1965;30:2900–2924.
28. Miyabe K. Evaluation of chromatographic performance of various packing materials having different structural characteristics as stationary phase for fast high performance liquid chromatography by new moment equations. *J Chromatogr A*. 2008;1183:49–64.
29. Ludlum DB, Warner RC, Smith HW. The diffusion of thiourea in water at 25 deg. *J Phys Chem*. 1962;66:1540–1542.
30. Dunlop PJ, Pepela CN, Steel BJ. Diffusion study at 25 deg. with a shearing diffusiometer. Comparison with the gouy and conductance methods. *J Am Chem Soc*. 1970;92:6743–6750.
31. Wilke CR, Chang P. Correlation of diffusion coefficients in dilute solutions. *AIChE J*. 1955;1:264–270.
32. Poling BE, Prausnitz JM, O' Connel JP. *The Properties of Gases and Liquids*, 5th ed. McGraw-Hill: New York, NY. 2001.
33. Li J, Carr PW. Accuracy of empirical correlations for estimating diffusion coefficients in aqueous organic mixtures. *Anal Chem.* 1997;69:2530–2536.
34. Foley JP, Dorsey JG. Equations for calculation of chromatographic figures of merit for ideal and skewed peaks. *Anal Chem.* 1983;55:730–737.
35. Gritti F, Kazakevich Y, Guiochon G. Effect of the surface coverage of endcapped C_{18}-silica on the excess adsorption isotherms of commonly used organic solvents from water in reversed phase liquid chromatography. *J Chromatogr A*. 2007;1169:111–124.
36. Cabooter D, Lynen F, Sandra P, Desmet G. Total pore blocking as an alternative method for the on-column determination of the external porosity of packed and monolithic reversed-phase columns. *J Chromatogr A*. 2007;1157:131–141.
37. Knox JH, McLaren L. A new gas chromatographic method for measuring gaseous diffusion coefficients and obstructive factors. *Anal Chem.* 1964;36:1477–1482.
38. Gritti F, Guiochon G. Effect of the surface coverage of C_{18}-bonded silica particles on the obstructive factor and intraparticle diffusion mechanism. *Chem Eng Sci*. 2006;61:7636–7650.
39. Miyabe K, Matsumoto Y, Guiochon G. Peak parking–moment analysis method as a strategy for studying the mass transfer in the stationary phase. *Anal Chem.* 2007;79:1970–1982.
40. Guiochon G, Martin M. Effects of a high pressure in liquid chromatography. *J Chromatogr A*. 2005;1090:16–38.
41. Tallareck U, Albert K, Bayer E, Guiochon G. Measurement of transverse and axial apparent dispersion coefficients in packed beds. *AIChE J*. 1996;42:3041–3064.
42. Kataoka T, Yoshida H, Ueyama K. Mass transfer in laminar region between liquid and packing material surface in the packed bed. *J Chem Eng Jpn*. 1972;5:132–136.
43. Farkas T, Sepaniak MJ, Guiochon G. Radial distribution of the flow velocity, efficiency and concentration in a wide HPLC column. *AIChE J*. 1997;43:1964–1974.
44. Farkas T, Guiochon G. Contribution of the radial distribution of the flow velocity to band broadening in HPLC columns. *Anal Chem.* 1997;69:4592–4600.
45. Martin M, Guiochon G. Influence of retention on band broadening in turbulent-flow liquid and gas chromatography. *Anal Chem.* 1982;54:1533–1540.
46. Aris R. On the dispersion of a solute in a fluid flowing through a tube. *Proc Roy Soc*. 1956;A235:67–77.
47. Broeckhoven K, Desmet G. Numerical and analytical solutions for the column length-dependent band broadening originating from axiaymmetrical trans-column velocity gradients. *J Chromatogr A*. 2009;1216:1325–1337.

Manuscript received Mar. 30, 2009, and revision received Aug. 7, 2009.